ZF Precoding-Based Spatial Domain SIC Method for MIMO Full Duplex Systems: A Performance Analysis Under CSI Errors

Xuan Chen, Vincent Savaux, Matthieu Crussière, Patrick Savelli, Kofi-Clément Yao

ZF Precoding-Based Spatial Domain SIC Method for MIMO Full Duplex Systems: A Performance Analysis Under CSI Errors

Xuan Chen*†‡, Vincent Savaux*, Matthieu Crussière†, Patrick Savelli* and Kofi-Clément Yao§
*b<>com, 1219 Av. des Champs Blancs, 35510 Cesson-Sévigné, France
†Univ. Rennes, INSA Rennes, CNRS, IETR UMR-6164, F-35700 Rennes, France
‡TDF, 155 bis Av. Pierre Brossolette, 92120 Montrouge, France
§Lab-STICC, CNRS, UMR 6285, UBO 29238 Brest, France

***Abstract*—In this paper, we evaluate the performance of a newly developed spatial domain zero-forcing (ZF) based self-interference cancellation (SIC) method in a generic multiple-input multiple-output (MIMO) full-duplex (FD) system. To this end, we theoretically evaluate the influence of channel state information (CSI) error on the SIC performance of our considered approach, and we validate our results through simulations. In particular, we show that the additional received self-interference (SI) power due to the CSI errors is quadratically proportional to a particular parameter α, quantifying the level of CSI errors. Furthermore, simulations results show that the increase of SI power has a negligible impact on the overall system performance in terms of spectral efficiency (SE), which proves the robustness of our considered SIC method.**

***Index Terms*—Channel state information, full-duplex, MIMO, self-interference cancellation, zero forcing precoding.**

I. Introduction

FULL DUPLEX (FD) has proven to be one of the most attractive technologies in wireless communication networks through the last decades. Its main advantage results in the simultaneous transmission and reception of different signals within the same frequency band, which allows any FD system to theoretically double the spectral efficiency (SE) compared to half duplex (HD) systems [1]–[4]. However, FD systems suffer from self-interference (SI) which unavoidably occurs since the receiver ($\mathrm{R_x}$) of the system is very likely to receive the transmitted signal from its own transmitter ($\mathrm{T_x}$), while the $\mathrm{R_x}$ is expecting to receive another signal. Thus, an efficient self-interference cancellation (SIC) method is mandatory for any FD system to work properly.

Recently, it has been suggested in [5] an easy-to-implement spatial domain zero-forcing (ZF) based SIC method which consists of using an additional radio frequency (RF) chain at $\mathrm{T_x}$ side dedicated to SI mitigation in a multiple input multiple output (MIMO) system architecture. The method has proven to be highly efficient in terms of SIC performance and enables an interference-free environment for the considered MIMO FD transceiver. However, similarly to [6], [7], a perfect channel state information (CSI) is considered in [5], which may be an overly idealistic assumption. In fact, in practice, the CSI should be considered as imperfect due to the CSI estimators and the presence of the additive noise. Thus, the robustness evaluation of FD systems under CSI errors such as in [8] and [9] is relevant.

In this paper, we suggest to evaluate the robustness of the SIC approach in [5] under CSI error in a generic MIMO FD system. Our contribution is twofold: first, we theoretically show that the considered SIC precoder under CSI error can be written as the sum of the original precoder without CSI error an additional erroneous precoder arising from the CSI error. Secondly, we theoretically prove that the increase in received SI power is quadratically proportional to a parameter α, reflecting the quality of channel estimation. Simulation results support our theoretical analysis and furthermore, it also shows that this increase in SI power has a negligible impact on the overall system performance in terms of SIC and SE, thus proving the robustness of the considered SIC approach.

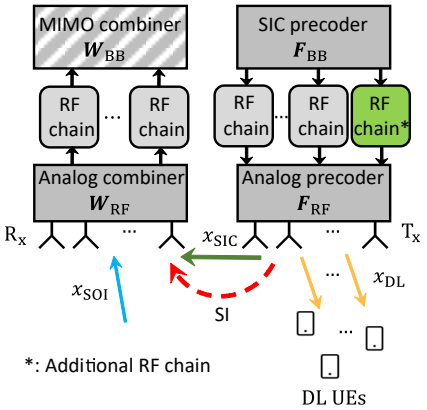

Fig. 1. Hybrid beamforming architecture of the considered MIMO FD system.

The rest of the paper is organized as follows: Section II presents the generic MIMO FD system transceiver model we consider, in particular the global input-output model, the spatial domain SIC hybrid beamforming model as well as the introduced CSI error model. Section III presents the theoretical analysis of the effect of the CSI errors on the considered SIC approach. Section IV presents the simulation results in accordance with our theoretical analysis and Section V concludes this paper.

II. System Model

A. Global Input-Output Model

The considered MIMO FD system transceiver model is presented in Fig. 1. In order to keep the model as generic as possible, we consider typical blocks of MIMO FD transceiver communication chain such as RF chains, analog RF beamformers (represented by the matrices $\boldsymbol{W}_{\mathrm{RF}}$ for the $\mathrm{R_x}$ side and $\boldsymbol{F}_{\mathrm{RF}}$

for the $\mathrm{T_x}$ side) and digital baseband (BB) beamformers (represented by the matrices $\boldsymbol{F}_{\mathrm{BB}}$ for the $\mathrm{T_x}$ side and $\boldsymbol{W}_{\mathrm{BB}}$ for the $\mathrm{R_x}$ side). During the FD operation of the considered transceiver, the $\mathrm{T_x}$ array transmits through $M_{\mathrm{T_x}}$ antennas K beams to a number of K devices, represented by user equipments (UEs) in our scenario. At the same time, the $\mathrm{R_x}$ array receives a signal of interest (SOI) coming from a third party, which can be either a UE for UL signal transmissions or another BS for a backhaul signal, through $\mathrm{M}_{\mathrm{R_x}}^{(\mathrm{BS})}$ antennas. Due to the simultaneous transmission and reception, the SI signal is inherently generated and disturbs the reception of the SOI at the $\mathrm{R_x}$ side. The core of the considered SIC method [5] is to consider the SI signal as another data stream within the FD system. To this end, we implement an additional RF chain at $\mathrm{T_x}$ whose role is to transmit a specific SIC signal x_{SIC} constructed as a linear combination of the transmitted signal x_{DL} and actively cancels the effect of the SI in the specific direction of the $\mathrm{R_x}$. The construction of this signal is done thanks to the design of the digital precoder $\boldsymbol{F}_{\mathrm{BB}}$, which is detailed hereafter. Note that the considered SIC method does not require any processing from the digital combiner $\boldsymbol{W}_{\mathrm{BB}}$. In our analysis, we assume $\boldsymbol{W}_{\mathrm{BB}}=\boldsymbol{I}$, to solely examine the SIC precoder $\boldsymbol{F}_{\mathrm{BB}}$ (hence the hatched part in Fig. 1). To simplify, we also assume that nearby UE devices are equipped with isotropic antennas, meaning they do not have the capability for analog or digital beamforming. The considered SIC approach operates by block, where the global MIMO communication channel, denoted by $\boldsymbol{H}$, is formed such that each block corresponds to a channel involved in the scenario. Consequently, we can consider all the receivers of this communication scenario as an equivalent receiver and gather them in a unique input-output relation. Thus, the received signal of the equivalent MIMO receivers of this scenario can be determined from Fig. 1 and is written as follows:

$$\boldsymbol{y}=\underbrace{\boldsymbol{W}_{\mathrm{RF,eq}}^{H}\boldsymbol{H}\boldsymbol{F}_{\mathrm{RF}}}_{\boldsymbol{H}_{\mathrm{eq}}}\boldsymbol{F}_{\mathrm{BB}}\boldsymbol{P}\boldsymbol{x}+\boldsymbol{W}_{\mathrm{RF,eq}}^{H}\boldsymbol{n}+\boldsymbol{y}_{\mathrm{SOI}}, \quad (1)$$

with $\boldsymbol{y}$ the vector of size $(K+1)\times 1$ gathering all the received beams of the scenario, including the $\mathrm{R_x}$ of the BS and the nearby downlink (DL) UEs. $\boldsymbol{H}=\boldsymbol{D}_{\beta}^{\frac{1}{2}}\odot\boldsymbol{G}$ represents the global MIMO channel matrix, where $\boldsymbol{G}$ is the normalized MIMO channel matrix and $\boldsymbol{D}_{\beta}$ represents the matrix capturing the effects of the path loss of each MIMO channel coefficient as in [10]. Matrix $\boldsymbol{H}$ is of size $(M_{\mathrm{R_x}}^{(\mathrm{BS})}+\sum_{k=0}^{K-1}M_{\mathrm{R_x}}^{(\mathrm{UE},k)})\times M_{\mathrm{T_x}}$, $M_{\mathrm{R_x}}^{(\mathrm{UE},k)}$ being the number of antennas of the kth DL UE. $\boldsymbol{H}_{\mathrm{eq}}=\boldsymbol{W}_{\mathrm{eq,RF}}^{H}\boldsymbol{H}\boldsymbol{F}_{\mathrm{RF}}$ represents the $(K+1)\times(K+1)$ equivalent channel matrix considering the effect of the analog beamformers $\boldsymbol{W}_{\mathrm{RF,eq}}$ and $\boldsymbol{F}_{\mathrm{RF}}$. $\boldsymbol{F}_{\mathrm{BB}}$ represents the SIC precoder of dimension $(K+1)\times K$, the design of which is detailed later. $\boldsymbol{x}$ is the vector of size $K\times 1$ gathering all the transmitted signal from the $\mathrm{T_x}$ of the BS, while $\boldsymbol{P}$ represents the $K\times K$ diagonal matrix regrouping the root square of the different allocated power for the transmission of each signal in $\boldsymbol{x}$. The vector of noise $\boldsymbol{n}$ is of size $(M_{\mathrm{R_x}}^{(\mathrm{BS})}+\sum_{k=0}^{K-1}M_{\mathrm{R_x}}^{(\mathrm{UE},k)})\times 1$ and gathers all the noise components at each antenna of all the receivers of the scenario. Finally, $\boldsymbol{y}_{\mathrm{SOI}}=[y_{\mathrm{SOI}},y_{\mathrm{int},0},...,y_{\mathrm{int},K-1}]^{T}$ is the vector of size $(K+1)\times 1$ with y_{SOI} the received SOI at $\mathrm{R_x}$ of the BS and $y_{\mathrm{int},k}$ $(\forall k\in\{0,...,K-1\})$ the cross interference the SOI may have on the kth UE. Note that we do not need to specify the model for the MIMO channel matrix $\boldsymbol{H}$ since the considered SIC strategy is valid for any channel model.

B. Analog Beamforming Model

In this paragraph, we specify the design of the analog beamformers. We choose to adopt a partially-connected RF chain structure for both $\mathrm{T_x}$ and $\mathrm{R_x}$ of the BS as in [5], which means the antennas dedicated to one RF chain are independent from the other RF chains. Since we deploy a uniform planar array (UPA) structure for our BS transceiver with a $\frac{\lambda}{2}$ spacing, the expression of the ith $(\forall i\in\{0,...,M_{\mathrm{T_x},k}-1\})$ coefficient of the steering vector pointing towards the kth UE $(\forall k\in\{0,...,K-1\})$ is given as follows:

$$\boldsymbol{e}_{k,i}^{(\mathrm{BS})}=\gamma e^{-j\pi(a_{k,i}\sin(\phi_k)+b_{k,i}\sin(\theta_k)\cos(\phi_k))}, \quad (2)$$

with $\gamma=\frac{1}{\sqrt{M_{\mathrm{T_x},k}}}$ the factor of normalization where $M_{\mathrm{T_x},k}$ corresponds to the total number of elementary antennas of the $\mathrm{T_x}$ dedicated to the kth UE, ϕ_k and θ_k corresponding to elevation and azimuth angles of each direction, $a_{k,i}$ and $b_{k,i}$ two positive integers indicating the vertical and horizontal position of the unitary radiating elements within the sub antenna array dedicated to the kth UE. By denoting $M_{k,V}^{(\mathrm{T_x})}$ (resp. $M_{k,H}^{(\mathrm{T_x})}$) the number of columns (resp. rows) of elementary antennas dedicated to the direction k on the $\mathrm{T_x}$ array, it naturally comes that $a_{k,i}$ (resp. $b_{k,i}$) takes value in $\{0,...,M_{k,V}^{(\mathrm{T_x})}-1\}$ (resp. $\{0,...,M_{k,H}^{(\mathrm{T_x})}-1\}$) and $M_{k,V}^{(\mathrm{T_x})}\times M_{k,H}^{(\mathrm{T_x})}=M_{\mathrm{T_x},k}$. Without loss of generality, we use a beamsteering technique to direct the beam straight towards the corresponding UE, as this represents the most suitable direction to maximize their received signal power. Note that other analog beamforming methods may be utilized to better leverage the NLOS propagation paths of the MIMO channel without impacting the results of our analysis in terms of SIC capability. For a matter of clarity, we note $\boldsymbol{e}_k$ instead of $\boldsymbol{e}_k(\phi_k,\theta_k)$ for all the steering vectors related to the $\mathrm{T_x}$ or $\mathrm{R_x}$ of the BS in the following. Furthermore, the steering vectors related to the BS are specified with the superscript (BS) (*e.g.* $\boldsymbol{e}_0^{(\mathrm{BS})}$ for the steering vector of the $\mathrm{T_x}$ antenna array pointing toward the first UE). The analog precoding matrix $\boldsymbol{F}_{\mathrm{RF}}$ of dimension $M_{\mathrm{T_x}}\times(K+1)$ is simply defined as a horizontal concatenation of different steering vectors dedicated to each RF chain:

$$\boldsymbol{F}_{\mathrm{RF}}=\begin{bmatrix}\boldsymbol{e}_{\mathrm{SIC}}^{(\mathrm{BS})} & \boldsymbol{0} & \cdots & \boldsymbol{0}\\ \boldsymbol{0} & \boldsymbol{e}_0^{(\mathrm{BS})} & \vdots & \boldsymbol{0}\\ \vdots & \vdots & \vdots & \vdots\\ \boldsymbol{0} & \cdots & \cdots & \boldsymbol{e}_{K-1}^{(\mathrm{BS})}\end{bmatrix}. \quad (3)$$

The definition of the analog combining matrix $\boldsymbol{W}_{\mathrm{RF,eq}}$ of dimension $(M_{\mathrm{R_x}}^{(\mathrm{BS})}+\sum_{k=0}^{K-1}M_{\mathrm{R_x}}^{(\mathrm{UE},k)})\times(K+1)$ is similar to $\boldsymbol{F}_{\mathrm{RF}}$. For more details regarding the definition of $\boldsymbol{W}_{\mathrm{RF,eq}}$ and $\boldsymbol{F}_{\mathrm{RF}}$, readers may refer to (18) and (11) in [5].

C. Considered Digital Beamforming Model

The expression of the considered $(K+1)\times K$ ZF-based SIC precoder $\boldsymbol{F}_{\mathrm{BB}}$ is first introduced in [5] and can be defined as follows:

$$\boldsymbol{F}_{\mathrm{BB}}=\boldsymbol{F}_{\mathrm{ZF}}=\frac{1}{\eta}(\boldsymbol{H}_{\mathrm{eq}}^{H}\boldsymbol{H}_{\mathrm{eq}})^{-1}\boldsymbol{H}_{\mathrm{eq}}^{H}\boldsymbol{A}_{\mathrm{ZF}}, \quad (4)$$

with $\eta=\|(\boldsymbol{H}_{\mathrm{eq}}^{H}\boldsymbol{H}_{\mathrm{eq}})^{-1}\boldsymbol{H}_{\mathrm{eq}}^{H}\boldsymbol{A}_{\mathrm{ZF}}\|_F$ the normalization factor and $\boldsymbol{A}_{\mathrm{ZF}}$ a $(K+1)\times K$ matrix defined as $\boldsymbol{A}_{\mathrm{ZF}}=[\boldsymbol{0},\boldsymbol{I}_K]^{T}$ with $\boldsymbol{0}$ a $K\times 1$ null vector whose role is to guarantee a perfect SIC as shown in [5] and $\boldsymbol{I}_K$ the $K\times K$ identity matrix. It is worth emphasizing that the presented system model (1)

using (4) may be idealistic as it considers a perfect CSI at the transmitter (through $\boldsymbol{F}_{\mathrm{BB}}$). In practice, it is likely that the overall channel $\boldsymbol{H}$ is not perfectly estimated due to the additive noise for instance, and imperfect channel estimators.

III. Theoretical analysis

A. CSI Error Model

We hereby present the CSI error model we consider. We assume that each channel coefficient of the MIMO channel matrix $\boldsymbol{H}$ suffers from an additive error for instance due to the channel estimator. Calling $\Delta\boldsymbol{H}$ the matrix of channel error, it comes that the channel matrix after including CSI errors $\boldsymbol{H}'$ can be defined as follows:

$$\boldsymbol{H}' = \boldsymbol{H} + \Delta\boldsymbol{H}, \tag{5}$$

where $\Delta\boldsymbol{H}$ is defined in a similar way to $\boldsymbol{H}$ as follows:

$$\Delta\boldsymbol{H} = \boldsymbol{D}_{\beta}^{\frac{1}{2}} \odot \boldsymbol{\Psi}, \tag{6}$$

The reason for this modeling choice is that the considered SIC method operates on $\boldsymbol{H}$, which is formed by block. Due to geometrical constraints, the different sub-channels within $\boldsymbol{H}$ naturally exhibit significantly different free-space path loss, resulting in widely varying orders of magnitude. On the other hand, $\boldsymbol{\Psi}$ is a matrix whose coefficient follows a commonly considered i.i.d. Gaussian variable-based model, as in [11], [12] (*i.e.* $\boldsymbol{\Psi}_{m,n} \sim \mathbb{C}\mathcal{N}(0,\alpha^2\frac{\sigma_{m,n}^2}{2})$). Note that in our model, the variance of the (m,n)th channel coefficient $\sigma_{m,n}^2$ corresponds to the power of the disturbance added to this coefficient, where α is a general parameter in [0;1] quantifying how noisy the channel estimation can be. In particular, $\alpha = 0$ corresponds to the case where there is no CSI error, which results from a perfect channel estimator. Conversely, $\alpha = 1$ denotes a critical point where the error variance's amplitude is similar to that of the channel, which may result from a very poor channel estimator. Note that the chosen range for α gives an arbitrary idea of the quality of the channel estimation. Eventually, if the estimated channel is excessively noisy, α may exceed 1.

B. Effect of Analog Beamforming

In this section, we theoretically analyze the robustness of the considered spatial domain SIC approach against CSI errors. For that purpose, we first define the equivalent channel matrix $\boldsymbol{H'}_{\mathrm{eq}}$ under CSI errors as follows:

$$\boldsymbol{H'}_{\mathrm{eq}} = \boldsymbol{W}_{\mathrm{RF,eq}}^{H}\boldsymbol{H'}\boldsymbol{F}_{\mathrm{RF}} = \boldsymbol{H}_{\mathrm{eq}} + \Delta\boldsymbol{H}_{\mathrm{eq}}, \tag{7}$$

where $\Delta\boldsymbol{H}_{\mathrm{eq}} = \boldsymbol{W}_{\mathrm{RF,eq}}^{H}\Delta\boldsymbol{H}\boldsymbol{F}_{\mathrm{RF}}$. Since the conventional matrix product only consists of linear operations, it can be easily deduced from (7) that the (m,n)th coefficient of the equivalent channel matrix $\Delta\boldsymbol{H}_{\mathrm{eq},m,n}$ follows a zero-mean Gaussian distribution as for $\boldsymbol{\Psi}_{m,n}$. We then denote $\nu_{m,n}^2$ the variance of $\Delta\boldsymbol{H}_{\mathrm{eq},m,n}$ which is constructed as a linear combination of $\sigma_{m,n}^2$ and depends on the different steering angles defined in (2) and the FD transceiver antenna numbers, so that each coefficient of the equivalent channel matrix obeys a centered Gaussian distribution (*i.e.* $\Delta\boldsymbol{H}_{\mathrm{eq},m,n} \sim \mathbb{C}\mathcal{N}(0,\alpha^2\nu_{m,n}^2)$). It is then worth noticing that the general parameter α can be extracted from the variance and thus leads to:

$$\Delta\boldsymbol{H}_{\mathrm{eq},m,n} = \alpha\Delta\boldsymbol{H''}_{\mathrm{eq},m,n}, \tag{8}$$

with $\Delta\boldsymbol{H''}_{\mathrm{eq},m,n}$ the coefficient of the mth row and nth column of the equivalent channel matrix with its error following a centered Gaussian distribution with variance $\nu_{m,n}^2$.

C. Considered ZF Precoder Under CSI Error

We now theoretically analyze the robustness of the previously defined ZF-based SIC method. To this end, we first evaluate the effect of the CSI error on $\boldsymbol{F}_{\mathrm{ZF}}$, which leads to the following proposition:

Proposition 1. *The considered ZF-based SIC precoder under CSI error can be approximated as follows:*

$$\boldsymbol{F'}_{\mathrm{ZF}} \approx \boldsymbol{F}_{\mathrm{ZF}} + \Delta\boldsymbol{F}_{\mathrm{ZF}}, \tag{9}$$

with $\boldsymbol{F}_{\mathrm{ZF}}$ defined as in (4) and $\Delta\boldsymbol{F}_{\mathrm{ZF}}$ defined as follows:

$$\begin{aligned}\Delta\boldsymbol{F}_{\mathrm{ZF}} = &-\frac{1}{\eta'}\boldsymbol{C}(\boldsymbol{H}_{\mathrm{eq}}^{H}\boldsymbol{H}_{\mathrm{eq}})^{-1}\boldsymbol{H}_{\mathrm{eq}}^{H}\boldsymbol{A}_{\mathrm{ZF}} \\ &+\frac{1}{\eta'}(\boldsymbol{H}_{\mathrm{eq}}^{H}\boldsymbol{H}_{\mathrm{eq}})^{-1}\Delta\boldsymbol{H}_{\mathrm{eq}}^{H}\boldsymbol{A}_{\mathrm{ZF}} \\ &-\frac{1}{\eta'}\boldsymbol{C}(\boldsymbol{H}_{\mathrm{eq}}^{H}\boldsymbol{H}_{\mathrm{eq}})^{-1}\Delta\boldsymbol{H}_{\mathrm{eq}}^{H}\boldsymbol{A}_{\mathrm{ZF}},\end{aligned} \tag{10}$$

where $\eta' = \|(\boldsymbol{H}_{\mathrm{eq}}^{'H}\boldsymbol{H'}_{\mathrm{eq}})^{-1}\boldsymbol{H}_{\mathrm{eq}}^{'H}\boldsymbol{A}_{\mathrm{ZF}}\|_F$ represents the new normalization factor taking into account the CSI errors, and $\boldsymbol{C}$ is defined as follows:

$$\begin{aligned}\boldsymbol{C} = &(\boldsymbol{H}_{\mathrm{eq}}^{H}\boldsymbol{H}_{\mathrm{eq}})^{-1}\boldsymbol{H}_{\mathrm{eq}}^{H}\Delta\boldsymbol{H}_{\mathrm{eq}} + (\boldsymbol{H}_{\mathrm{eq}}^{H}\boldsymbol{H}_{\mathrm{eq}})^{-1} \\ &\Delta\boldsymbol{H}_{\mathrm{eq}}^{H}\boldsymbol{H}_{\mathrm{eq}} + (\boldsymbol{H}_{\mathrm{eq}}^{H}\boldsymbol{H}_{\mathrm{eq}})^{-1}\Delta\boldsymbol{H}_{\mathrm{eq}}^{H}\Delta\boldsymbol{H}_{\mathrm{eq}}.\end{aligned} \tag{11}$$

Proof. We first derive the expression of the ZF digital precoder under CSI errors $\boldsymbol{F'}_{\mathrm{ZF}}$ from (4) as follows:

$$\boldsymbol{F'}_{\mathrm{ZF}} = \frac{1}{\eta'}(\boldsymbol{H'}_{\mathrm{eq}}^{H}\boldsymbol{H'}_{\mathrm{eq}})^{-1}\boldsymbol{H'}_{\mathrm{eq}}^{H}\boldsymbol{A}_{\mathrm{ZF}}. \tag{12}$$

By replacing $\boldsymbol{H'}_{\mathrm{eq}}$ by its definition in (7) and by factorising by $\boldsymbol{H}_{\mathrm{eq}}^{H}\boldsymbol{H}_{\mathrm{eq}}$, (12) can be further developed as:

$$\begin{aligned}\boldsymbol{F'}_{\mathrm{ZF}} = &\frac{1}{\eta'}(\boldsymbol{H}_{\mathrm{eq}}^{H}\boldsymbol{H}_{\mathrm{eq}} + \boldsymbol{H}_{\mathrm{eq}}^{H}\Delta\boldsymbol{H}_{\mathrm{eq}} + \Delta\boldsymbol{H}_{\mathrm{eq}}^{H}\boldsymbol{H}_{\mathrm{eq}} \\ &+\Delta\boldsymbol{H}_{\mathrm{eq}}^{H}\Delta\boldsymbol{H}_{\mathrm{eq}})^{-1}(\boldsymbol{H}_{\mathrm{eq}}^{H} + \Delta\boldsymbol{H}_{\mathrm{eq}}^{H})\boldsymbol{A}_{\mathrm{ZF}} \\ = &\frac{1}{\eta'}(\boldsymbol{I}+\boldsymbol{C})^{-1}(\boldsymbol{H}_{\mathrm{eq}}^{H}\boldsymbol{H}_{\mathrm{eq}})^{-1}(\boldsymbol{H}_{\mathrm{eq}}^{H} + \Delta\boldsymbol{H}_{\mathrm{eq}}^{H})\boldsymbol{A}_{\mathrm{ZF}},\end{aligned} \tag{13}$$

with $\boldsymbol{C}$ defined as in (11). Furthermore, as our CSI error models in (6) suggests, each $\Delta\boldsymbol{H}_{m,n}$ includes the order of magnitude of $\boldsymbol{H}_{m,n}$. When multiplied by $\nu_{m,n}^2$, it comes that the order of magnitude of the eigenvalues of $\boldsymbol{C}$ depend only on the order of magnitude of $\nu_{m,n}^2$. To further simplify (13), we adopt the following assumption:

Assumption 1. *The values of each $\sigma_{m,n}^2$ is considered to be small enough so that all the eigenvalues $\lambda_{\boldsymbol{C},i}$ of $\boldsymbol{C}$ have their module smaller than 1: $\forall i \in \{0,...,K\}, |\lambda_{\boldsymbol{C},i}| < 1$.*

Then, it results that $\boldsymbol{F'}_{\mathrm{ZF}}$ can be further approximated with Neumann series as in [13], which leads to:

$$\boldsymbol{F'}_{\mathrm{ZF}} = \frac{1}{\eta'}\sum_{n=0}^{+\infty}(-1)^n\boldsymbol{C}^n(\boldsymbol{H}_{\mathrm{eq}}^{H}\boldsymbol{H}_{\mathrm{eq}})^{-1}(\boldsymbol{H}_{\mathrm{eq}}^{H} + \Delta\boldsymbol{H}_{\mathrm{eq}}^{H})\boldsymbol{A}_{\mathrm{ZF}}. \tag{14}$$

Similarly, we assume that the values of $\sigma_{m,n}^2$ are small enough so that the following assumption may hold to further simplify (14):

Assumption 2. *In the development of $\boldsymbol{C}^n$, the second and higher order terms are negligible in front of the first order terms: $\Delta\boldsymbol{H}_{\mathrm{eq}}^{H}\Delta\boldsymbol{H}_{\mathrm{eq}} << \Delta\boldsymbol{H}_{\mathrm{eq}}$.*

Considering assumption 2, (14) then becomes:

$$\boldsymbol{F'}_{\mathrm{ZF}} \approx \frac{1}{\eta'}(\boldsymbol{I}-\boldsymbol{C})(\boldsymbol{H}_{\mathrm{eq}}^{H}\boldsymbol{H}_{\mathrm{eq}})^{-1}(\boldsymbol{H}_{\mathrm{eq}}^{H} + \Delta\boldsymbol{H}_{\mathrm{eq}}^{H})\boldsymbol{A}_{\mathrm{ZF}}. \tag{15}$$

Some simple arrangements of (15) lead to (9) which concludes the proof. □

Interestingly, it can be noticed that the ZF-based digital precoder under erroneous CSI is the sum of 2 terms: the first one $\boldsymbol{F}_{\mathrm{ZF}}$ corresponds to the ZF-based digital precoder under perfect CSI, and the term $\Delta\boldsymbol{F}_{\mathrm{ZF}}$ is induced by the CSI error. It is foreseeable that the final result of the digital precoding $\boldsymbol{H}_{\mathrm{eq}}\boldsymbol{F'}_{\mathrm{ZF}}$ is also a sum of two terms: the first one $\boldsymbol{H}_{\mathrm{eq}}\boldsymbol{F}_{\mathrm{ZF}}$ where the SI is effectively canceled, and the second one $\boldsymbol{H}_{\mathrm{eq}}\Delta\boldsymbol{F}_{\mathrm{ZF}}$ which represents the main source of distortion for the overall system performance besides the noise.

D. Received SI Power Under CSI Error

Now we evaluate the received SI power with the previously described ZF-based digital precoder under CSI error.

Proposition 2. *The received SI power P'_{SI} under the erroneous ZF-based precoder $\boldsymbol{F'}_{\mathrm{ZF}}$ is quadratically proportional to the general parameter α and takes the following form:*

$$P'_{\mathrm{SI}}=\alpha^2\sum_{j=0}^{K-1}\mathbb{E}\left[\left|(\boldsymbol{A})_{0,j}-(\boldsymbol{B}^*)_{0,j}\right|^2\right], \tag{16}$$

with $\boldsymbol{A}$ and $\boldsymbol{B}$ defined as follows:

$$\boldsymbol{A}=\frac{1}{\eta'}\boldsymbol{H}_{\mathrm{eq}}(\boldsymbol{H}_{\mathrm{eq}}^H\boldsymbol{H}_{\mathrm{eq}})^{-1}\Delta\boldsymbol{H''}_{\mathrm{eq}}^H\boldsymbol{A}_{\mathrm{ZF}}\boldsymbol{P}, \tag{17}$$

$$\boldsymbol{B}=\frac{1}{\eta'}\boldsymbol{H}_{\mathrm{eq}}(\boldsymbol{H}_{\mathrm{eq}}^H\boldsymbol{H}_{\mathrm{eq}})^{-1}$$
$$(\boldsymbol{H}_{\mathrm{eq}}^H\Delta\boldsymbol{H''}_{\mathrm{eq}}+\Delta\boldsymbol{H''}_{\mathrm{eq}}^H\boldsymbol{H}_{\mathrm{eq}})(\boldsymbol{H}_{\mathrm{eq}}^H\boldsymbol{H}_{\mathrm{eq}})^{-1}\boldsymbol{H}_{\mathrm{eq}}^H\boldsymbol{A}_{\mathrm{ZF}}\boldsymbol{P}. \tag{18}$$

Proof. By replacing $\boldsymbol{C}$ by its definition in (11) and by applying assumption 2, (10) can be simplified as follows:

$$\Delta\boldsymbol{F}_{\mathrm{ZF}}=-\frac{1}{\eta'}(\boldsymbol{H}_{\mathrm{eq}}^H\boldsymbol{H}_{\mathrm{eq}})^{-1}(\boldsymbol{H}_{\mathrm{eq}}^H\Delta\boldsymbol{H}_{\mathrm{eq}}+\Delta\boldsymbol{H}_{\mathrm{eq}}^H\boldsymbol{H}_{\mathrm{eq}})$$
$$(\boldsymbol{H}_{\mathrm{eq}}^H\boldsymbol{H}_{\mathrm{eq}})^{-1}\boldsymbol{H}_{\mathrm{eq}}^H\boldsymbol{A}_{\mathrm{ZF}}+\frac{1}{\eta'}(\boldsymbol{H}_{\mathrm{eq}}^H\boldsymbol{H}_{\mathrm{eq}})^{-1}\Delta\boldsymbol{H}_{\mathrm{eq}}^H\boldsymbol{A}_{\mathrm{ZF}}. \tag{19}$$

It is worth remarking that in each of the terms of (19) there is the matrix $\Delta\boldsymbol{H}_{\mathrm{eq}}$. Considering (8), we define $\Delta\boldsymbol{F''}_{\mathrm{ZF}}$ such that $\Delta\boldsymbol{F}_{\mathrm{ZF}}=\alpha\Delta\boldsymbol{F''}_{\mathrm{ZF}}$ to emphasize the influence of the general parameter α. At this point, the ZF-based digital precoder based on erroneous CSI can be rewritten as follows:

$$\boldsymbol{F'}_{\mathrm{ZF}}=\boldsymbol{F}_{\mathrm{ZF}}+\alpha\Delta\boldsymbol{F''}_{\mathrm{ZF}}. \tag{20}$$

Now we calculate the received SI power with the previously calculated ZF precoder to evaluate the influence of the CSI error on the overall system performance. By performing the conventional matrix product in (1), the contribution of SI is naturally gathered in the first row of the resulting matrix $\boldsymbol{H}_{\mathrm{eq}}\boldsymbol{F'}_{\mathrm{ZF}}\boldsymbol{P}$. Furthermore, by considering normalized i.i.d. symbols transmitted from the BS and the linearity of the expectation, the received SI power can be defined as follows:

$$P'_{\mathrm{SI}}=\sum_{j=0}^{K-1}\mathbb{E}\left[\left|(\boldsymbol{H}_{\mathrm{eq}}\boldsymbol{F'}_{\mathrm{ZF}}\boldsymbol{P})_{0,j}\right|^2\right]. \tag{21}$$

In order to calculate (21), we first calculate the general expression of the matrix product $\boldsymbol{H}_{\mathrm{eq}}\boldsymbol{F'}_{\mathrm{ZF}}\boldsymbol{P}$, which leads to:

$$\boldsymbol{H}_{\mathrm{eq}}\boldsymbol{F'}_{\mathrm{ZF}}\boldsymbol{P}=\boldsymbol{H}_{\mathrm{eq}}\boldsymbol{F}_{\mathrm{ZF}}\boldsymbol{P}+\boldsymbol{H}_{\mathrm{eq}}\alpha\Delta\boldsymbol{F''}_{\mathrm{ZF}}\boldsymbol{P}$$
$$=\boldsymbol{R}_{\mathrm{ZF}}+\alpha\boldsymbol{A}-\alpha\boldsymbol{B}, \tag{22}$$

with $\boldsymbol{R}_{\mathrm{ZF}}=\boldsymbol{H}_{\mathrm{eq}}\boldsymbol{F}_{\mathrm{ZF}}\boldsymbol{P}$ the resulting matrix of the equivalent channel matrix with the ZF precoding matrix without CSI error. The matrices $\boldsymbol{A}$ and $\boldsymbol{B}$ are defined as in (17) and (18), respectively. From (22) the received SI power for the jth RF chain at $\mathrm{R_x}$ ($\forall j\in\{0,\ldots,K-1\}$) side can be expressed as follows:

$$\left|(\boldsymbol{H}_{\mathrm{eq}}\boldsymbol{F'}_{\mathrm{ZF}}\boldsymbol{P})_{0,j}\right|^2=\left|(\boldsymbol{R}_{\mathrm{ZF}})_{0,j}\right|^2$$
$$+2\alpha\left(\Re\Big((\boldsymbol{R}_{\mathrm{ZF}})_{0,j}(\boldsymbol{A}^*)_{0,j}\Big)-\Re\Big((\boldsymbol{R}_{\mathrm{ZF}})_{0,j}(\boldsymbol{B}^*)_{0,j}\Big)\right)$$
$$+\alpha^2\left(\left|(\boldsymbol{A})_{0,j}-(\boldsymbol{B}^*)_{0,j}\right|^2\right). \tag{23}$$

We know that the ZF digital precoder is able to carry out perfect SIC when there is no CSI error, which means that the coefficients of the entire first row of the resulting matrix $\boldsymbol{R}_{\mathrm{ZF}}$ are equal to 0 as it is shown in [5]. Thus, (23) can be simplified as:

$$\left|(\boldsymbol{H}_{\mathrm{eq}}\boldsymbol{F'}_{\mathrm{ZF}}\boldsymbol{P})_{0,j}\right|^2=\alpha^2\left(\left|(\boldsymbol{A})_{0,j}-(\boldsymbol{B}^*)_{0,j}\right|^2\right). \tag{24}$$

By simply inserting (24) into (21), one can easily recognize (16) which concludes the proof. □

From (16), we observe that the received SI power under CSI error P'_{SI} can be written as the product between α^2 and a matrix dependent on $\boldsymbol{A}$ and $\boldsymbol{B}$. While α physically represents the quality of channel estimation, $\boldsymbol{A}$ and $\boldsymbol{B}$ do not depend on α and represent the mathematical consequence capturing the effect of each intrinsic variance $\sigma^2_{m,n}$ of the error matrix $\boldsymbol{\Psi}$. We can conclude from (16) that the received SI power under presence of CSI error is quadratically proportional to α. Simulations results from the next Section would validate our theoretical analysis.

IV. Simulations and Discussion

A. Simulations Parameters

In our simulation, we consider a generic FD transceiver with an UPA structure for both $\mathrm{R_x}$ and $\mathrm{T_x}$. The $\mathrm{T_x}$ side deploys $10\times 4=40$ elementary antennas connected to 5 RF chains (8 antennas per RF chain) to transmit 5 beams (including the one to perform SIC) in different elevation and azimuth angles with a total transmission power of 10W, while the $\mathrm{R_x}$ side deploys 8 elementary antennas to receive a SOI from a target located 100m from the FD transceiver. We consider that the target deploys 8 elementary antennas with a transmission power of 0.1W. The FD transceiver's working frequency is set at 28GHz with a bandwidth of 400MHz, which is a typical 5G NR working condition as in [14].

B. Simulation Results

We first evaluate in Fig. 2 the influence of the general parameter α on the received SI power P'_{SI}. Specifically, we compare the theoretical expression of the received SI power in (16) and the simulated SI power defined in (21). We first observe in Fig. 2 that the amplitude of the received SI power for both the simulated and theoretical result is very low (less than 1 nW) across all considered values of $\sigma^2_{m,n}$. Considering a base station transmitting with a power of 10W, we can conclude that even under CSI errors, the considered ZF-based SIC method can still effectively carry out SIC. Furthermore, we note that the increment of SI power behaves similarly for both theoretical and simulated results across all chosen values of $\sigma^2_{m,n}$. Specifically, our theoretical result for $\sigma^2_{m,n}=0.01$ only differs from the simulated one for α higher than 0.8, while the difference is more pronounced for higher values of $\sigma^2_{m,n}$ (beginning at $\alpha=0.7$ for $\sigma^2_{m,n}=0.03$ and at $\alpha=0.6$ for $\sigma^2_{m,n}=0.05$). This difference may be attributed to our assumptions 1 and 2 in the

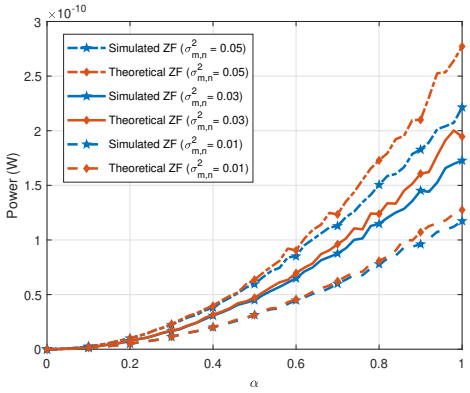

Fig. 2. Theoretical and simulated received SI power P'_{SI} (in W) versus α for different values of $\sigma^2_{m,n}$ for the ZF-based SIC method under faulty CSI.

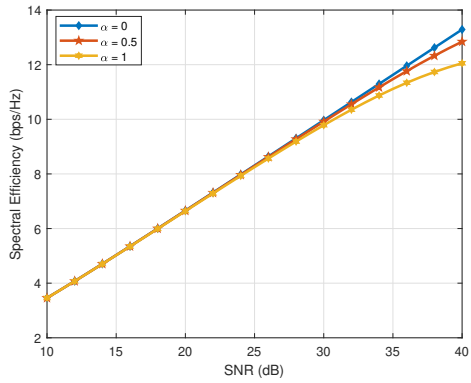

Fig. 3. Comparison of SE for the reception of SOI vs SNR under different level of CSI error: perfect CSI $\alpha=0$, average CSI error $\alpha=0.5$, worst case CSI $\alpha=1$ ($\sigma^2_{m,n}=0.01$).

calculation of (16), which becomes slightly inaccurate as the value of $\sigma^2_{m,n}$ increases. However, the overall result shows that the received SI power is quadratically proportional to the general parameter α, thereby validating our theoretical developments.

Next in Fig. 3, we assess the considered MIMO FD system's performance in terms of the SE of the SOI under different levels of CSI error (*i.e.* $\alpha=0$, $\alpha=0.5$ and $\alpha=1$) versus the SNR for $\sigma^2_{m,n}=0.01$. The SE is computed over 2000 realizations, generating both the error matrix $\boldsymbol{\Psi}$ and the multipath channels involved in $\boldsymbol{H}$ each time. The SE can be defined as follows:

$$\mathrm{SE}=\log_2\left(1+\frac{P_{\mathrm{SOI}}}{P'_{\mathrm{SI}}+P_{\mathrm{N}}}\right), \tag{25}$$

with P_{SOI} the received SOI power and P_{N} the received noise power and the SNR is defined as $\mathrm{SNR}=\frac{P_{\mathrm{SOI}}}{P_{\mathrm{N}}}$. From Fig. 3, the behavior of the $\alpha=0.5$ and $\alpha=1$ cases closely resembles that of the perfect CSI case ($\alpha=0$), with only a slight degradation due to CSI erro noticeable from SNR = 30 dB onwards. Specifically, we observe a degradation of approximately 1 bps/Hz between the $\alpha=1$ and the $\alpha=0$ cases at SNR = 40 dB, while only a minor difference of less than 0.5 bps/Hz is evident between the $\alpha=0$ and the $\alpha=0.5$ cases at SNR = 40 dB. This result aligns with our expectations, given the low amplitude of the received SI power from Fig. 2. We can conclude here that the considered ZF-based digital SIC precoder is effectively robust against CSI error, enabling proper operation for various MIMO FD systems.

V. Conclusion

In this paper, we assess the robustness of a ZF-based digital precoder under CSI error in a generic MIMO FD transceiver. We show through theory and simulation that the increase of SI power due to the CSI error varies quadratically with the parameter α, aiming at qualifying the SI power directly from the quality of the channel estimator. Moreover, this increase in CSI error does not have any significant impact on the performance of the FD transceiver in terms of SIC and SE. Thus, the robustness of the considered SIC approach is proved, showing its promising capability to be implemented in any MIMO FD system.

References

[1] A. Sabharwal, P. Schniter, D. Guo, D. Bliss, S. Rangarajan, and R. Wichman, "In-Band Full-Duplex Wireless: Challenges and Opportunities," *IEEE Journal on Selected Areas in Communications*, vol. 32, 11 2013.

[2] G. Liu, F. R. Yu, H. Ji, V. C. M. Leung, and X. Li, "In-Band Full-Duplex Relaying: A Survey, Research Issues and Challenges," *IEEE Commun. Surveys Tuts.*, vol. 17, no. 2, pp. 500–524, 2015.

[3] H. Alves, T. Riihonen, and H. Suraweera, Eds., *Full-Duplex Communications for Future Wireless Networks*. Springer Singapore, 2020.

[4] T. Dinc and H. Krishnaswamy, "Millimeter-wave full-duplex wireless: Applications, antenna interfaces and systems," in *2017 IEEE Custom Integrated Circuits Conference (CICC)*, 2017, pp. 1–8.

[5] X. Chen, V. Savaux, and P. Savelli, "Spatial Domain based Self-Interference Cancellation Techniques in Full-Duplex Massive MIMO Systems," *techrXiv*, 9 2023.

[6] Z. He, W. Xu, H. Shen, D. W. K. Ng, Y. C. Eldar, and X. You, "Full-duplex communication for isac: Joint beamforming and power optimization," *IEEE Journal on Selected Areas in Communications*, vol. 41, no. 9, pp. 2920–2936, 2023.

[7] C. K. Sheemar, G. C. Alexandropoulos, D. Slock, J. Querol, and S. Chatzinotas, "Full-Duplex-Enabled Joint Communications and Sensing with Reconfigurable Intelligent Surfaces," in *2023 31st European Signal Processing Conference (EUSIPCO)*, 2023, pp. 1509–1513.

[8] B. C. Nguyen, P. V. Tri, X. N. Tran, and L. T. Dung, "SER performance of MIMO full-duplex relay system with channel estimation errors and transceivers hardware impairments," *AEU - International Journal of Electronics and Communications*, vol. 136, p. 153751, 2021.

[9] B. C. Nguyen, N. N. Thang, X. N. Tran, and L. T. Dung, "Impacts of Imperfect Channel State Information, Transceiver Hardware, and Self-Interference Cancellation on the Performance of Full-Duplex MIMO Relay System," *Sensors*, vol. 20, no. 6, 2020.

[10] A. Roze, M. Hélard, M. Crussière, and C. Langlais, "Millimeter-Wave Digital Beamsteering in Highly Line-Of-Sight Environments for Massive MIMO Systems," in *WWWRF35 Meeting*, Copenhague, Denmark, Oct. 2015. [Online]. Available: https://univ-rennes.hal.science/hal-01252090

[11] X. Huang, A. Tuyen Le, and Y. J. Guo, "Transmit Beamforming for Communication and Self-Interference Cancellation in Full Duplex MIMO Systems: A Trade-Off Analysis," *IEEE Transactions on Wireless Communications*, vol. 20, no. 6, pp. 3760–3769, 2021.

[12] D. Mi, M. Dianati, L. Zhang, S. Muhaidat, and R. Tafazolli, "Massive MIMO Performance With Imperfect Channel Reciprocity and Channel Estimation Error," *IEEE Transactions on Communications*, vol. 65, no. 9, pp. 3734–3749, 2017.

[13] K. B. Petersen and M. S. Pedersen, "The matrix cookbook," nov 2012, version 20121115.

[14] A. Bishnu, M. Holm, and T. Ratnarajah, "Performance Evaluation of Full-Duplex IAB Multi-Cell and Multi-User Network for FR2 Band," *IEEE Access*, vol. 9, pp. 72 269–72 283, 2021.